Dyes and Pigments 94 (2012) 1–9

Contents lists available at SciVerse ScienceDirect

Dyes and Pigments

journal homepage: www.elsevier.com/locate/dyepig

Removal of acid dyes from aqueous media by adsorption onto amino-functionalized nanoporous silica SBA-3

Mansoor Anbia*, Samira Salehi

Research Laboratory of Nanoporous Materials, Faculty of Chemistry, Iran University of Science and Technology, Narmak, Tehran 16846, Iran

ARTICLE INFO

Article history:
Received 3 June 2011
Received in revised form
5 October 2011
Accepted 23 October 2011
Available online 15 November 2011

Keywords:
Adsorption
Acid dyes
Amino-functionalized SBA-3
Mesoporous
Freundlich isotherm
Nano adsorbent

ABSTRACT

Adsorption of acid dyes on SBA-3 ordered mesoporous silica, ethylenediamine functionalized SBA-3 (SBA-3/EDA), aminopropyl functionalized SBA-3 (SBA-3/APTES) and pentaethylene hexamine functionalized SBA-3 (SBA-3/PEHA) materials has been studied. The structural order and textural properties of the synthesized materials have been studied by XRD, FT-IR and nitrogen adsorption–desorption analysis. The adsorption capacity of the adsorbents varies in the following order: SBA-3/PEHA > SBA-3/APTES > SBA-3/EDA > SBA-3. The SBA-3/PEHA is found to have the highest adsorption capacity for all acid dyes. The adsorption mechanism which is based on electrostatic attraction and hydrogen bonding is described. Batch studies were performed to study the effect of various experimental parameters such as chemical modification, contact time, initial concentration, adsorbent dose, agitation speed, solution pH and reaction temperature on the adsorption process. The Langmuir and Freundlich isotherm models have been applied and the Freundlich model was found to be fit with the equilibrium isotherm data. Kinetics of adsorption follows the second-order rate equation.

1. Introduction

Acid dyes are used in many industries such as textile, paper, food processing, cosmetics, plastics, printing, leather, pharmaceutical and dye manufacturing. Water pollution caused by industrial wastewater has become a common problem for many countries [1–3]. It is reported that over 100,000 different commercial dyes and pigments exist, and each year over 7×10^5 ton of dyestuffs is produced. About 1–20% of the total world production of dyes is lost during dyeing process and therefore a large quantity of the dyes appear in wastewater [4,5]. Removal of dyes from water is very important because the water quality is greatly affected by colour and even the presence of very small concentrations of dyes (less than 1 mg L^{-1}) in water is highly visible and is considered unpleasant. Besides that, many of these dyes also cause health problems such as allergic dermatitis, skin irritation, cancer and mutation in human [6–8].

A wide range of methods including biological and physico-chemical technologies have been used for removing coloured contaminants from wastewater to decrease their impact on the environment. The main treatment processes include: oxidation or ozonation [9,10], coagulation and flocculation [11], membrane separation [12] and adsorption [13,14]. Among the numerous techniques of dye removal, adsorption has been found to be the most convenient and effective, and it is also less expensive than the others. This process transfers the species from the water effluent to a solid phase thereby keeping the effluent volume to a minimum [15]. During the past few years new promising adsorbents have been reported to be used in adsorption process [16–25].

Mesoporous materials, such as SBA-3 [26,27], ammonium functionalized MCM-41 [28], and silane-modified HMS [29], have been found to be as suitable adsorbents for the removal of dyes from wastewater.

These materials are typically prepared in the presence of surfactant, which act as template during sol–gel hydrothermal synthesis and they are characterized by uniform and controlled adjusted pore sizes, by high specific surface areas and by long-range order [30–32]. A large variety of mesoporous silica has been synthesized by using several templates under various conditions and the formation mechanism of the mesostructures has also been studied by some research groups [31,33–36].

In 1998, Zhao et al. [37] synthesized a new type of mesoporous material called SBA, with uniform hexagonal structure. SBA-3-typemesoporous molecular sieves were synthesized using a low molecular weight alkyl quaternary ammonium template room temperature and under acidic condition. SBA-3 has been shown to possess some micropores inside their mesopore walls, which may be served as active sites for modification [38–40].

A well established fact is that SBA-3 has a negative charge density due to the presence of Si–O and Si–OH groups, which

* Corresponding author. Tel.: +98 21 77240516; fax: +98 21 77491204.
E-mail address: anbia@iust.ac.ir (M. Anbia).

0143-7208/$ – see front matter © 2011 Elsevier Ltd. All rights reserved.
doi:10.1016/j.dyepig.2011.10.016

makes it unsuitable for adsorption of acid dyes because of the negative charge of these dyes. Functionalization of the silica surface with organic groups is very important and the effectiveness of SBA-3 in adsorption process can be improved by functionalizing the main network with functional groups suitable to adsorbe negative charged dyes [41,42].

In the present study, various amine functional groups have been studied for functionalization of the SBA-3 to enhance acid dyes adsorption, in view of the high affinity and interaction between the amine groups and acid dyes. The improvement in acid dyes adsorption is due to electrostatic attraction and hydrogen bonding between the surface of the adsorbent and acid dyes. The change in surface characteristics and pore structure of synthesized materials are characterized with FT-IR, XRD and nitrogen adsorption–desorption isotherms. The effect of various parameters on the removal of acid dyes such as chemical modification, contact time, initial concentration, adsorbent dose, agitation speed, solution pH and reaction temperature have been studied in detail. The equilibrium data are fitted into Langmuir and Freundlich equations to determine the correlation between the isotherm models and experimental data. The experimental data was also analyzed using the kinetic constants and first- and second-order kinetic models were calculated.

2. Experimental

2.1. Synthesis of SBA-3

The preparation procedure was taken from the literature [43]. The SBA-3 samples were synthesized using tetraethyl orthosilicate (TEOS, Merck) as the silica source and cetyltrimethylammonium bromide (CTAB, Merck) as template. The HCl aqueous solution (37%) was used to adjust the pH value of the reaction system. In a typical synthesis, 1 g of CTAB was dissolved in 47 mL of deionized water and acidified with 15 mL of HCl to obtain clear solution. TEOS (4.45 mL) was then added dropwise to the acidic CTAB solution stirring at 400 rpm at 30 °C, then the solution was left for 1 h. A white precipitate was recovered by filtration and washed with deionized water and dried at 100 °C overnight. Subsequently, the surfactant was removed by calcination at 550 °C in air for 5 h, increasing the temperature to 550 °C at 1 °C/min of the heating rate.

2.2. Synthesis of SBA-3 functionalized with APTES

2 g of 3-aminopropyl trimethoxysilane (APTES, Merck) was mixed with 2 g of SBA-3 in 60 mL of anhydrous toluene (for 10 h under reflux conditions and a nitrogen atmosphere). The resulting precipitate was filtered, washed with dichloromethane and ethanol, and was dried. It was then extracted with a soxhlet setup with a mixture of dichloromethane and ethanol with the ratio of 1:1 (V/V) to remove the remaining silylating reagent and was then vacuum-dried at 70 °C. The product obtained was denoted as SBA-3/APTES.

2.3. Synthesis of SBA-3 functionalized with PEHA

1 g of pentaethylene hexamine (PEHA, Merck) was dissolved in 50 g ethanol under stirring for 40 min at room temperature, and then 2 g SBA-3 was added. After refluxing for 4 h, the resulting mixture was evaporated at 80 °C. Finally, the samples were dried in air for 1 h at 100 °C and denoted as SBA-3/PEHA.

2.4. Synthesis of SBA-3 functionalized with EDA

For the preparation of SBA-3/EDA, a similar process to that of the SBA-3/PEHA was used and PEHA was replaced by ethylenediamine (EDA, Merck).

2.5. Characterization

The porosity characteristics of the mesoporous silica sorbents were determined by N_2 adsorption–desorption experiments performed at 77 K on micromeritics model ASAP 2010 sorptometer. The specific surface area (S_{BET}) was determined from the linear part of the Brunaure–Emmet–Teller (BET) equation. Pore size distribution was estimated from the adsorption branch of the isotherm by the Barrett–Joyner–Halenda (BJH) method.

The Fourier transform infrared spectra for the unfunctionalized and functionalized silica materials were measured on a DIGILAB FTS 7000 instrument under attenuated total reflection (ATR) mode using a diamond module.

X-ray diffraction (XRD) was used to identify the crystal phases of the mesoporous silica materials. These experiments were carried out on a Philips 1830 diffractometer equipped with Cu-Kα radiation. XRD patterns were obtained from 1° to 10° of 2θ, with a 2θ step size of 0.018° and a step time of 1 s.

2.6. Adsorption studies

Adsorption behaviour was studied by a batch method, which permits convenient evaluation of parameters that influence the adsorption process such as chemical modification, contact time, initial concentration, adsorbent dose, agitation speed, solution pH and reaction temperature. A series of aqueous solutions of acid dyes (the chemical structures and characteristics of the selected acid dyes are listed in Table 1) with the same pH and their concentration ranging from 20 to 150 mg L^{-1} were prepared by dissolving pure samples of the solutes in double distilled water, specifically. In each adsorption experiment, 5 mg adsorbent was added in 25 mL acid dyes solutions. The solutions were stirred continuously at constant to observe the effect of pH, acid dyes with the same initial concentration was adjusted to different pH (3–10) using 0.1 mol L^{-1} NaOH and 0.1 mol L^{-1} HCl solutions. To study the effect of temperature the adsorption was carried out at four different temperatures (20, 40, 60 and 80 °C) and for contact time studies the samples were taken at predetermined time intervals (15, 30, 45, 60, 90 and 120 min). The effect of agitation speed on the adsorption of acid dyes was carried out by varying the agitation speed from 50 to 300 rpm. After adsorption, the residual concentration of acid dyes in the filtrate was subsequently determined using the spectrophotometer at the wavelength corresponding to the maximum absorbance. The UV spectrophotometer was calibrated against standard solution before each analysis. The amount of acid dyes adsorbed per unit mass of the q_e (mg g^{-1}) was calculated by the following equation:

$$q_e = \frac{(C_0 - C_e)V}{W} \quad (1)$$

Where q_e is the adsorption capacity (mg g^{-1}) of the adsorbent at equilibrium; C_0 and C_e are the initial and equilibrium concentrations of solute (mg L^{-1}), respectively; V is the volume of the aqueous solution (L) and W is the mass (g) of adsorbent used in the experiments.

2.7. Adsorption kinetics of acid dyes

Adsorption kinetics experiments were made to investigate the effect of contact time and to determine the kinetic parameters. The adsorption kinetics of organic compound onto adsorbent were investigated at one fixed initial concentration of acid dyes (100 mg L^{-1}) by adding 25 mL acid dyes solution to 0.005 g of adsorbent. The solution was stirred continuously (150 rpm) at 25 °C. The samples at different time intervals (0–120 min) were

Table 1
List of selected acid dyes investigated in this study.

Generic name	Abbreviation	Molecular formula	Structure	λ_{max} (nm)
Acid Blue 113	AB-113	$C_{32}H_{21}N_5Na_2O_6S_2$	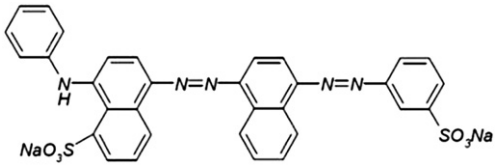	567
Acid Red 114	AR-114	$C_{37}H_{28}N_4Na_2O_{10}S_3$	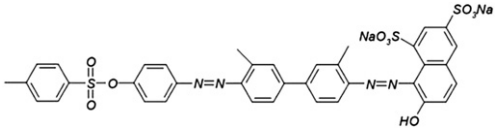	527
Acid Green 28	AG-28	$C_{34}H_{32}N_2Na_2O_{10}S_2$	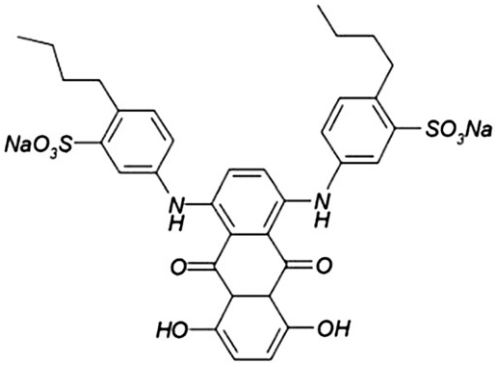	416
Acid Yellow 127	AY-127	$C_{26}H_{20}Cl_2N_9NaO_4S$	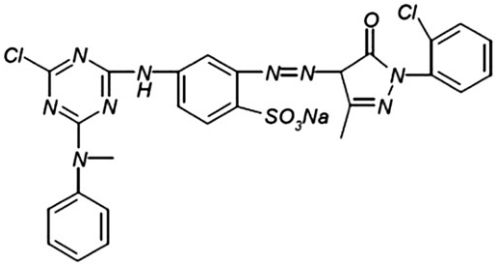	400
Acid Orange 67	AO-67	$C_{26}H_{21}N_4NaO_8S_2$	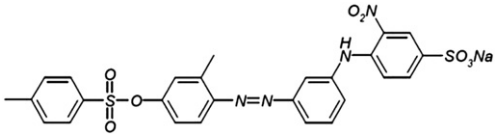	436

taken and filtered. The residual concentration of AR-114, AB-113, AG-28, AY-127 and AO-67 in the filtrate was measured and the adsorption amount (q_t) was calculated by the following equation:

$$q_t = \frac{(C_0 - C_t)V}{W} \quad (2)$$

Where q_t is the measure of adsorption at time t, C_0 is the initial concentration of acid dyes in the solution, C_t is the concentration of acid dyes in the solution at time t, V is the volume of the solution, and W is the mass of SBA-3/PEHA.

3. Results and discussion

3.1. Characterization of adsorbents

X-ray diffractograms for SBA-3 as well as functionalized silica materials are presented in Fig. 1. The XRD patterns display three peaks at $2\theta = 2.76^\circ$, 4.74° and 5.30° respectively. These peaks were indexed as (100), (110) and (200) crystal facets, which belong to one-dimensional hexagonal (P6 m) mesostructures. It must be noted that the amino-functionalized SBA-3 materials maintained the three peaks (at d spacing 100, 110 and 200) of the XRD pattern with reduced intensity compared with that for SBA-3. The intensity decrease of diffraction peaks indicates tdypi_3491_gr5_3c.tif - e lowering of mesopore uniformity. Moreover, the XRD patterns of SBA-3 materials demonstrate that hexagonally ordered structure of SBA-3 was persistent after the functionalization.

N_2 adsorption–desorption isotherms of unfunctionalized and amino-functionalized SBA-3 materials are presented in Fig. 2. SBA-3 materials show three distinct regions of N_2 adsorption isotherms. The initial part of the isotherm indicates a high "knee", followed by a slower growth in the adsorbed volume at low relative pressures (>0.1 P/P_0), may be attributed to a monolayer-multilayer adsorption on the pore walls. The high "knee" may illustrate the presence of the micropores inside SBA-3. At a relative pressure P/P_0 between 0.2 and 0.3, the isotherm exhibits a sharp step characteristic of capillary condensation within the mesopores. These isotherms show no hysteresis loop between adsorption and desorption branches, similar to that reported in the literature [44]. A very slow linear increase at higher relative pressures (>0.3 P/P_0) shows the adsorption on the outer surface of SBA-3. The overview features of

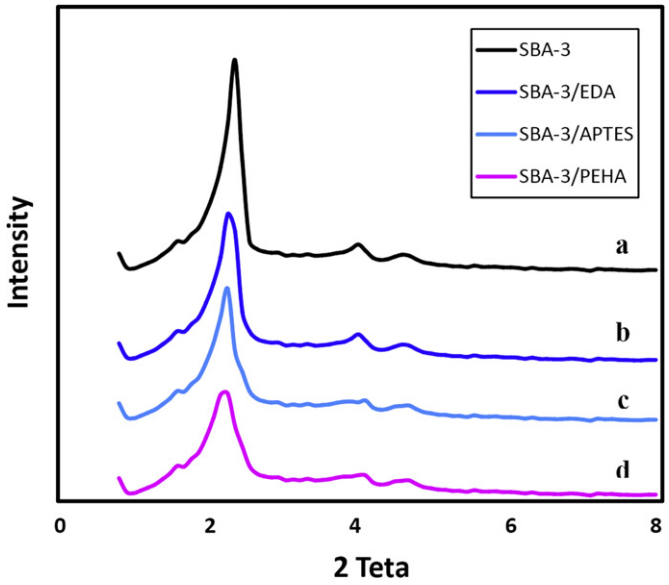

Fig. 1. XRD patterns of SBA-3 (a), SBA-3/EDA (b), SBA-3/APTES (C) and SBA-3/PEHA (d).

these isotherm scan be explained as the superposition of type I (for micropore) and type IV (for mesopore) isotherms [45].

The Brunauer-Emmett–Teller (BET) surface area, pore volumes and average pore diameter for each sample are listed in Table 2. The pure silica sample displayed much higher BET surface area, average pore diameter and pore volume when compared to the amino-functionalized SBA-3 materials. Introduction of amino functional groups into SBA-3 structure resulted in decrease of textural parameters.

Qualitative identification of functional groups was accomplished by FT-IR spectroscopy. Fig. 3 shows the FT-IR spectrum of unfunctionalized and amino-functionalized SBA-3 materials over the range of 4000–400 cm^{-1}. A broad band in the range of 3700–3010 cm^{-1} is seen which can be attributed to the framework of Si–OH group interaction with the defect sites and adsorbed water molecules. The Si–OH peak appears at about 3460 cm^{-1}, while peaks for the weak single Si–OH groups derived from the germinal Si–OH groups were observed at 3740 cm^{-1}. The asymmetric stretching vibrations of Si–O–Si and Si–OH are observed by the absorption bands at 1000–1360 cm^{-1} and the band at 790 cm^{-1} is assigned to free silica. In general, the functionalized silicas with

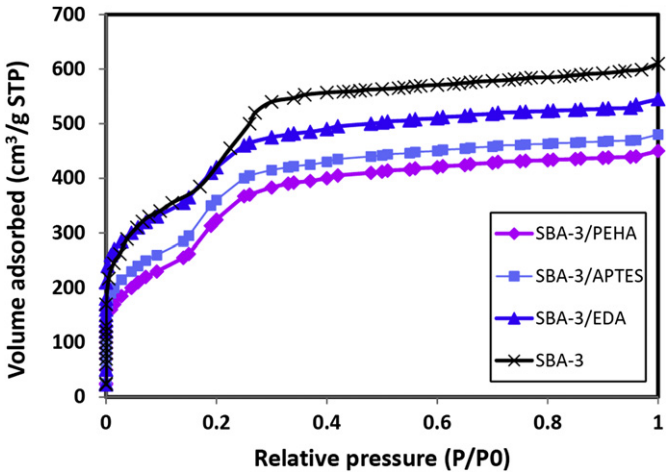

Fig. 2. Adsorption–desorption isotherms of nitrogen at 77 K on SBA-3, SBA-3/EDA, SBA-3/APTES and SBA-3/PEHA.

Table 2
Textural properties determined from nitrogen adsorption–desorption experiments at 77 K.

Adsorbent	ABET (m^2 g^{-1})	Average pore size (Å)	V_p (cm^3 g^{-1})
SBA-3	1435	21.6	0.96
SBA-3/EDA	1290	19.2	0.82
SBA-3/APTES	1092	16.8	0.67
SBA-3/PEHA	1005	16.3	0.62

amino groups show a broad NH_2 stretching at 3250–3450 cm^{-1}, an N–H deformation peak at 1640–1560 cm^{-1}, C–H stretching of methyl groups at 3000–2850 and 1450 cm^{-1}. The symmetric and asymmetric stretching vibrations of the $-NH_2$ groups appear at 3250–3450 cm^{-1} but in the spectrum of amino-functionalized SBA-3 materials are probably masked by the broad peak due to adsorbed water molecules. In addition, in comparison with the SBA-3/PEHA, the amino bands are weaker for SBA-3/APTES and SBA-3/EDA.

3.2. Effect of various parameters on adsorption

In the present study, SBA-3/PEHA was used for acid dyes removal from aqueous solutions. The effect of various important parameters such as contact time, initial concentration, adsorbent dose, agitation speed, solution pH and reaction temperature were investigated.

3.2.1. Effect of chemical modification

In order to evaluate the efficacy of the prepared adsorbents, the equilibrium adsorption of the acid dyes was studied as a function of equilibrium concentration. The adsorption isotherms of acid dyes on the adsorbents are shown in Figs. 4–8. The order of adsorption in terms of the amount adsorbed (mg/g adsorbent) on the adsorbents is: SBA-3/PEHA > SBA-3/APTES > SBA-3/EDA > SBA-3. In general, the adsorption capacity depends on the chemical and physical properties of the surface of adsorbent. Pure silica surface does not provide strong adsorption sites to interact strongly with acid dyes due to the fact that the hydroxyl groups on the silica surface fail to induce strong interactions with acid dyes. The adsorption capacity of acid dyes by mesoporous silica was enhanced through functionalization with amine groups. It is clear from the figures that the SBA-3/PEHA possessed a higher adsorption capacity towards acid dyes than that of the other adsorbents. The higher adsorption capacity of SBA-3/PEHA may be explained to proceed via electrostatic interaction and hydrogen bond formation

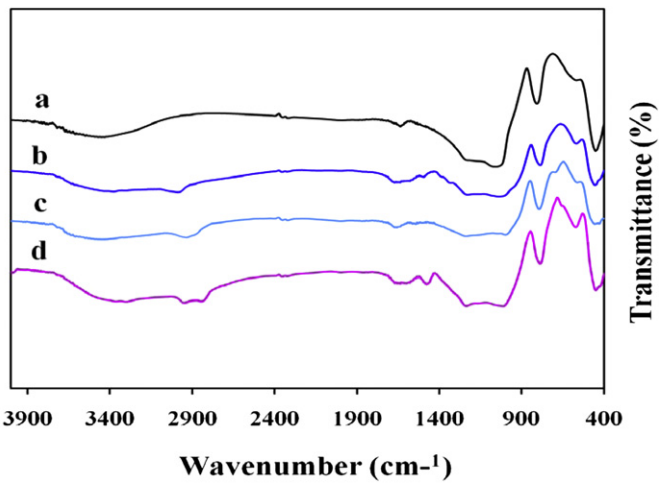

Fig. 3. FT-IR spectra of SBA-3 (a), SBA-3/EDA (b), SBA-3/APTES (C) and SBA-3/PEHA (d).

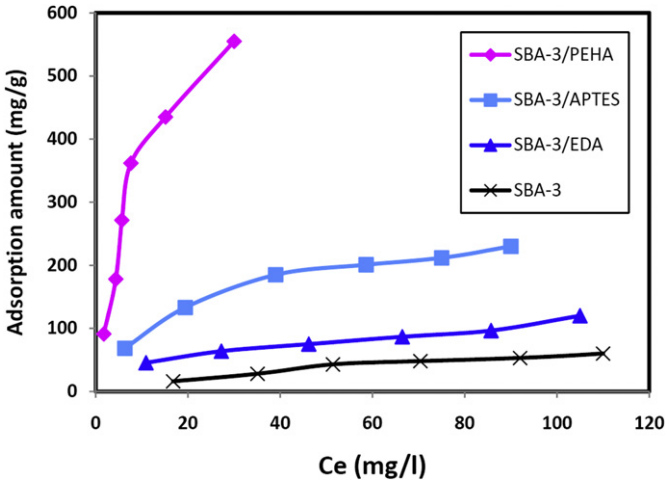

Fig. 4. Adsorption isotherm for: AB-113 adsorption on adsorbents (contact time = 60 min, adsorbent dosage = 0.2 g L^{-1}, pH = 6).

between the surface of the adsorbent and acid dyes. In the aqueous solution, the sulfonate groups of the dye dissociate and are converted to anionic ions. Also, in the presence of H^+, the amine groups of SBA-3/PEHA become protonated. Then the electrostatic attraction could occur between the positively charged protonated amino groups on the silica surface ($-NH_3^+$) and the negatively charged sulfonate groups ($-SO_3^-$) of the acid dyes. Besides that, a great distinction of the acid dyes is the number of hydrophilic functional groups, which have a strong tendency to form hydrogen bonds with SBA-3/PEHA. A simulation of interactions between SBA-3/PEHA and AG-28 is shown in Fig. 9.

It can be seen that hydrogen bonds between AG-28 and SBA-3/PEHA are formed by NH and = O, which can result in an increase of the adsorption. According to these results, SBA-3/PEHA was chosen as the adsorbent for the adsorption of acid dyes in this study.

3.2.2. Effect of contact time

The equilibrium time between the pollutant and the adsorbent is of significant importance in the wastewater treatment by adsorption. For an adsorbent to be efficient in wastewater treatment, it needs to be able to show a rapid uptake of the pollutants and reach the equilibrium in a short time. Adsorption equilibrium time is determined as the time after which the concentration of the acid dyes solution remain unchanged during the course of

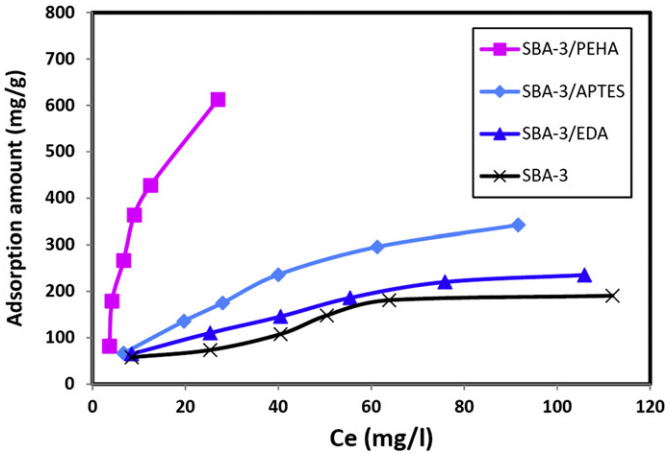

Fig. 5. Adsorption isotherm for: AR-114 adsorption on adsorbents (contact time = 60 min, adsorbent dosage = 0.2 g L^{-1}, pH = 6).

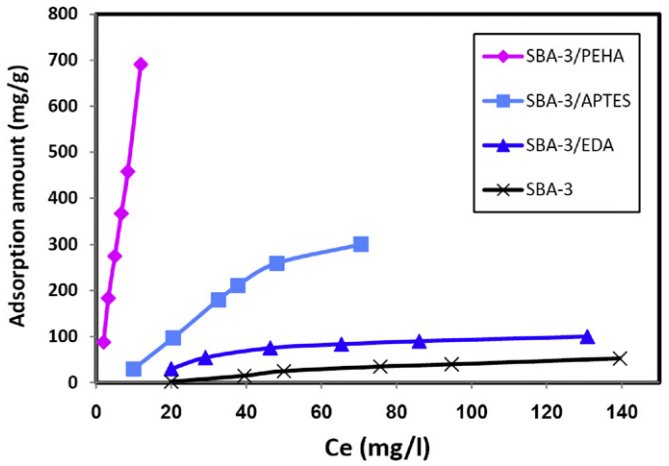

Fig. 6. Adsorption isotherm for: AG-28 adsorption on adsorbents (contact time = 60 min, adsorbent dosage = 0.2 g L^{-1}, pH = 6).

adsorption process. The effect of contact time on the adsorption of the acid dyes on SBA-3/PEHA is illustrated in Fig. 10. It is clear from the figure that acid dyes uptake is rapid in the first 15 min, after that proceeds at a slower rate, and finally reaches equilibrium at the end of 60 min. Therefore, optimum contact time for the adsorbent was found to be 60 min. The rapid uptake at the initial contact time can be attributed to the availability of the positively charged surface of SBA-3/PEHA and the slow rate of acid dye adsorption is probably due to the slow pore diffusion of the solute ion into the bulk of the adsorbent. In physical adsorption, most of the adsorption occurs within a short time of the contact.

3.2.3. Effect of initial concentration

A higher initial acid dye concentration leads to an increase in the mass gradient between the solution and the SBA-3/PEHA, which then functions as a driving force for the transfer of acid dye molecules from bulk solution to the SBA-3/PEHA surface. Effect of initial concentration on the uptake of acid dyes was studied at different initial concentrations (C_0 = 20–150 mg/L), keeping other parameters constant. As can be seen in Fig. 11, the adsorption capacity increases with increase of initial acid dyes concentration. The reason may be that the increase in the number of analyte molecules (or ions) competing for the available binding sites on the surface of the adsorbent. In addition, increase of initial acid dye concentration increases the number of collisions between acid dye anions and adsorbent, which enhances the sorption process.

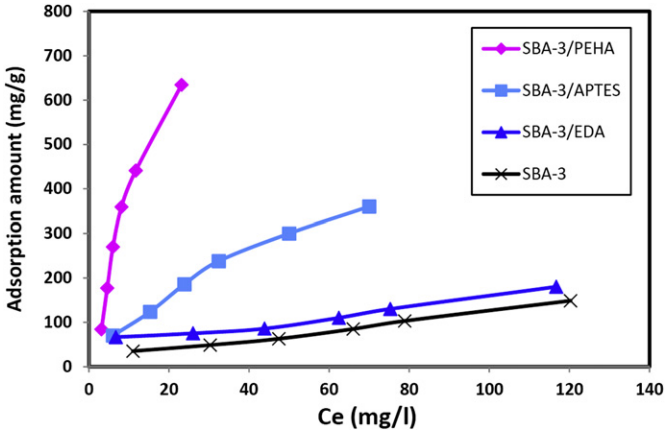

Fig. 7. Adsorption isotherm for: AY-127 adsorption on adsorbents (contact time = 60 min, adsorbent dosage = 0.2 g L^{-1}, pH = 6).

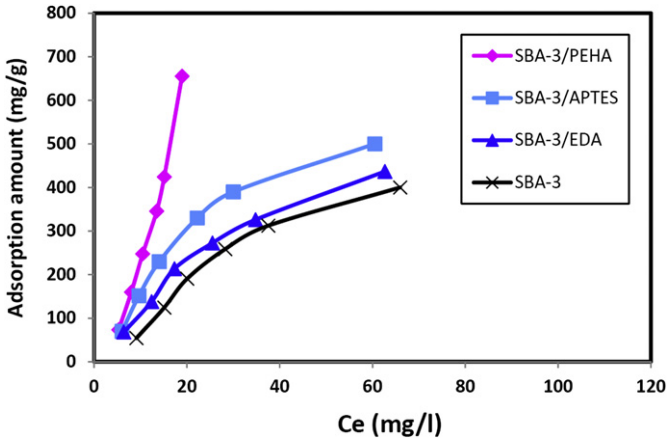

Fig. 8. Adsorption isotherm for: AO-67 adsorption on adsorbents (contact time = 60 min, adsorbent dosage = 0.2 g L^{-1}, pH = 6).

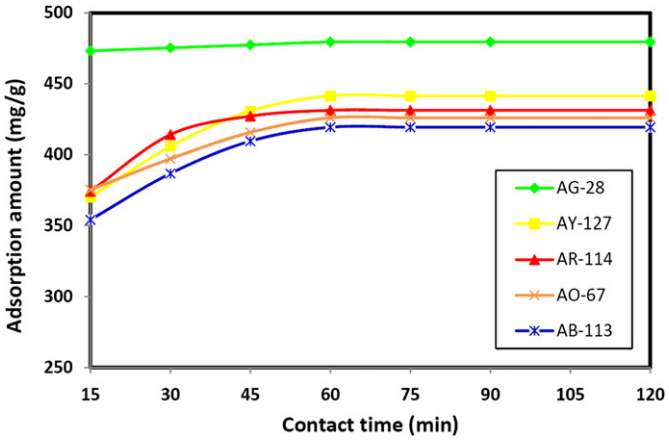

Fig. 10. Effect of contact for adsorption of acid dyes on SBA-3/PEHA (initial concentration = 100 mg L^{-1}, adsorbent dosage = 0.2 g L^{-1}, pH = 6).

3.2.4. *Effect of adsorbent dose*

The influence of adsorbent amount on acid dyes adsorption by SBA-3/PEHA is showed in Table 3. Adsorbent dose is an important parameter in determination of adsorption capacity and adsorption percent. The results indicated that at constant concentration of acid dyes by increasing the adsorbent contents from 0.2 to 0.4 g/L, the adsorption percent increases but adsorption capacity decreases. An increase in adsorption percent can be attributed to increased surface area and the availability of more adsorption sites whereas the decrease in adsorption capacity is due to the fact that some of the adsorption sites remain unsaturated during the adsorption process.

3.2.5. *Effect of agitation speed*

Agitation speed is an important parameter in adsorption phenomena, influencing the distribution of the solute in the bulk. The effect of agitation speed on removal efficiency of acid dyes was studied by varying the speed of agitation from 0 (without shaking) to 300 rpm, while keeping the analyte concentration and contact time constant. As shown in Fig. 12 the efficiency of acid dyes removal increased with increasing agitation speed from 0 rpm to 150 rpm and the adsorption capacity remained constant for agitation rates greater than 150 rpm. Increasing the agitation rate causes the film resistance to mass transfer surrounding the adsorbent particles to decrees, resulting in an increase in the adsorption of the dye molecules. The agitation speed of 150 rpm was selected as optimum speed.

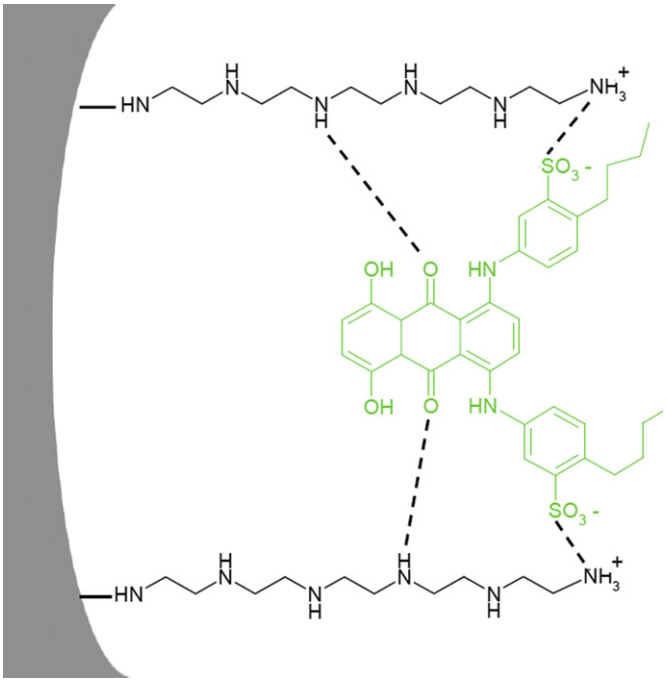

Fig. 9. Main interactions between AG-28 and SBA-3/PEHA.

3.2.6. *Effect of pH*

The pH of the solution affects the surface charge of the adsorbent and also the degree of ionization of the materials present in the solution. Increase in the solution pH causes the dissociation of the functional groups on the adsorbent surface active sites which in turn affects the adsorptive process. For studying the effect of pH on the adsorption capacity of SBA-3/PEHA, solutions were prepared in the pH range of 3.0–10.0. The pH of solutions were adjusted by 0.1 mol L^{-1} HCl or 0.1 mol L^{-1} NaOH. The adsorption capacity of SBA-3/PEHA increased with increase in solution pH and the maximum adsorption capacity for acid dyes was observed at pH 3 as depicted in Fig. 13. Acid dyes are also called anionic dyes because of they usually exist in the sulphate form. Therefore, at lower pH, the SBA-3/PEHA surface will be positively charged via protonation process, which increases the electrostatic attractions between acid dyes molecules and SBA-3/PEHA surface. At higher pH the number of positively charged sites are reduced and raised the number of negatively charged sites, creating electrostatic repulsion between the negatively charged surface of the SBA-3/PEHA and the anionic acid dyes molecules. On the other hand, the lower adsorption of

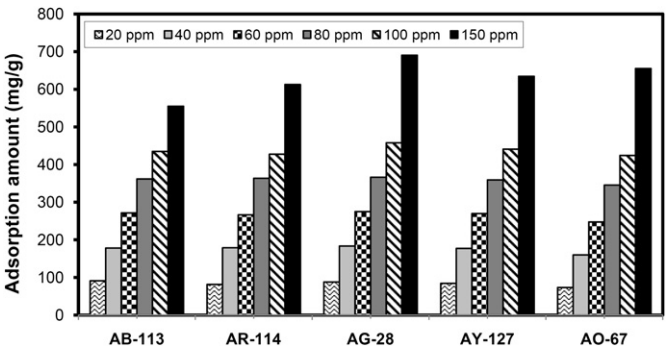

Fig. 11. Effect of initial concentration on adsorption of acid dyes on SBA-3/PEHA (contact time = 60 min, adsorbent dosage = 0.2 g L^{-1}, pH = 6).

Table 3
The adsorption percent and adsorption capacity of acid dyes.

Adsorbent dose (g/L)	AG-28		AY-127		AR-114		AO-67		AB-113	
	q_e (mg/g)	Adsorption percent (%)	q_e (mg/g)	Adsorption percent (%)	q_e (mg/g)	Adsorption percent (%)	q_e (mg/g)	Adsorption percent (%)	q_e (mg/g)	Adsorption percent (%)
0.2	479.55	95.91	441.45	88.29	427.5	85.5	418.9	83.78	419.3	83.86
0.3	305	97.6	287.06	91.86	580.71	89.83	278.87	89.24	274.31	87.78
0.4	247.17	98.87	236.8	94.72	231.07	92.43	234.02	93.61	234.17	93.67

acid dyes, at alkaline pH is because of the presence of excess OH^- ions competing with the dye anions for the adsorption sites. As a result, there was in a significant reduction in the adsorption of acid dyes from the solution. A similar behaviour was observed for the adsorption of anionic dye onto native and modified fungus biomass [46].

3.2.7. *Effect of temperature*

The adsorption studies were carried out at 20, 40, 60 and 80 °C and the results of these experiments are shown in Fig. 14. Temperature is a highly significant parameter in the adsorption process. It can be seen from the figure that decrease in temperature generally increase the adsorption capacity and maximum adsorption capacity is noticed at 20 °C which shows an exothermic adsorption. This may be due to the physical bonding between acid dye molecules and the active sites of the adsorbent. It is weakened as temperature increased, whereas, the solubility of dyes increased thus interaction forces between the solute and the solvent become stronger than those between solute and adsorbent, making the solute more difficult to adsorb. The adsorption is favoured by a decrease in temperature, a phenomenon which is also characteristic of physical adsorption.

3.3. *Adsorption isotherms*

The equilibrium of adsorption is one of the important physicochemical aspects for the evaluation of the sorption process as a unit operation. The distribution of solute between the solid and liquid phases is a measure of the distribution coefficient in the adsorption process and can be shown by the Freundlich and Langmuir equations. The Langmuir adsorption [47] is based on the assumption that adsorption occurs at specific homogeneous sites within the adsorbent and once a dye molecule occupies a site, no further adsorption takes place at that site. Moreover, Langmuir's model of adsorption depends on the assumption of monolayer adsorption on a structurally homogeneous adsorbent, where all the sorption sites are identical and energetically equivalent. The intermolecular forces decrease rapidly with distance and can be used to predict the existence of monolayer coverage of the adsorbate at the outer surface of the adsorbent. The linear form of the Langmuir isotherm equation is:

$$\frac{C_e}{q_e} = \frac{1}{qm^b} + \frac{1}{q_m}C_e \tag{3}$$

Where q_e is the amount of adsorbate adsorbed per unit mass of adsorbent (mg/g), C_e is the equilibrium concentration of the adsorbate (mg/L). q_m (mg g^{-1}) and b (L mg^{-1}) are the Langmuir constants related to maximum monolayer adsorption capacity and energy change in adsorption, respectively.

The Freundlich isotherm model [48] is an empirical equation assuming that the adsorption process takes place on heterogeneous surfaces and is not restricted to the formation of the monolayer. The Freundlich model considers different affinities for the binding sites on the adsorbent surface with interactions between the adsorbed molecules. This isotherm also considers that the sites with stronger affinity are occupied first. Its linearized form is given as:

$$\ln q_e = \ln K_F + \left(\frac{1}{n}\right)\ln C_e \tag{4}$$

where q_e is the amount of adsorbate adsorbed per unit mass of adsorbent (mg/g), C_e is the equilibrium concentration of the adsorbate (mg/L), K_F ($mg^{1-1/n}$ $L^{1/n}$ g) and n are Freundlich constants with n giving an indication of how favourable the adsorption process is and K_F is the adsorption capacity of the adsorbent. When ln q_e is plotted against ln C_e and the data are treated by linear regression analysis, K_F and $1/n$ constants are determined from the slope and intercept. The values of n and K_F can indicate whether the adsorption process is favourable or unfavourable. The fit of a model

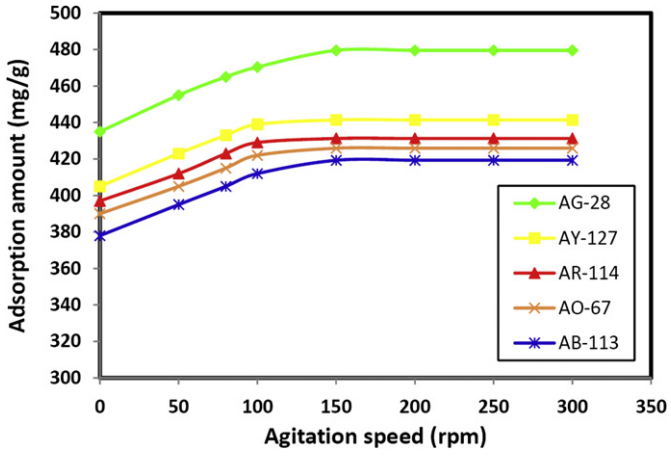

Fig. 12. Effect of agitation speed on of acid dyes by SBA-3/PEHA (initial concentration = 100 mg L^{-1}, contact time = 60 min, adsorbent dosage = 0.2 g L^{-1}, pH = 6).

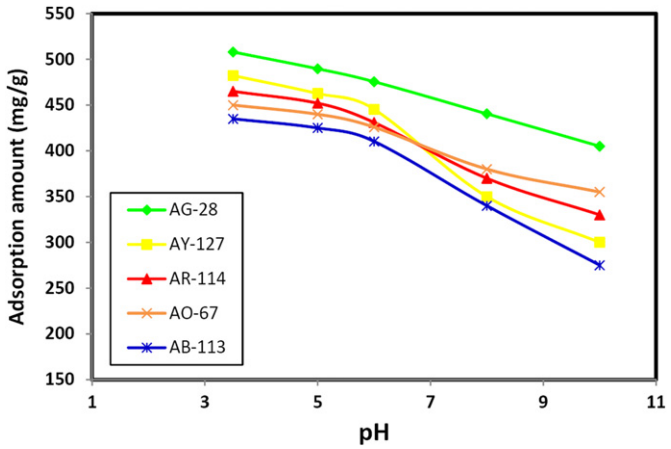

Fig. 13. Effect of pH on adsorption of acid dyes on SBA-3/PEHA (initial concentration = 100 mg L^{-1}, contact time = 60 min, adsorbent dosage = 0.2 g L^{-1}).

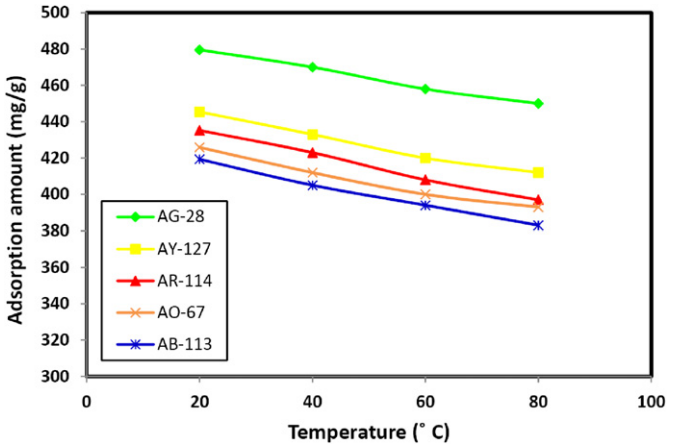

Fig. 14. Effect of temperature on adsorption of acid dyes on SBA-3/PEHA (initial concentration = 100 mg L^{-1}, contact time = 60 min, adsorbent dosage = 0.2 g L^{-1}, pH = 6).

to the experimental data are usually evaluated in terms of linear regression analysis where the R^2 value is used as an indication for the goodness of model fit with respect to R^2 values (Table 4), the adsorption of acid dyes on the SBA-3/PEHA can be evaluated as a process that mainly follows the Freundlich model. The magnitude of K_F and n values of Freundlich model showed easy uptake of acid dyes with a high adsorption capacity of adsorbent.

Values of $n > 1$ for acid dyes molecules indicates positive cooperativity in binding and a heterogeneous nature of adsorption (Table 4).

3.4. Adsorption kinetics

The mechanism of adsorption is important for the efficiency of the process, thus making a study of adsorption kinetics desirable. Any adsorption process is normally controlled by three diffusion steps: (i) transport of the solute from bulk solution to the film surrounding the adsorbent, (ii) from the film to the adsorbent surface, (iii) from the surface to the internal sites followed by binding of the metal ions to the active sites. The overall rate of the adsorption process is determined by the slowest step and usually it is thought that the step (ii) leads to surface adsorption and the step (iii) leads to intra-particle adsorption [49]. Several kinetic models can be used to express the mechanism of solute sorption onto a sorbent. In this work, pseudo-first-order and pseudo-second-order kinetic models were tested.

The pseudo-first-order kinetic model has been widely used to express the kinetics of acid dyes adsorption. A linear form of pseudo-first order kinetic was described by Lagergren [50]:

$$\log(q_e - q_t) = \log q_e - \left(\frac{K_1}{2,303}\right)t \quad (5)$$

Table 4
Isotherm parameters for adsorption of acid dyes on SBA-3/PEHA.

Dye	Langmuir			Freundlich		
	q_m (mg/g)	b (L/mg)	R^2	K_F (mg/g)	n (L/mg)	R^2
AG-28	3333	0.0184	0.9902	42.70	1.04	0.9921
AY-127	1250	0.0487	0.9688	52.24	1.20	0.9726
AR-114	1000	0.0571	0.9659	68.29	1.47	0.9762
A0-67	2500	0.0123	0.9751	48.49	1.12	0.9906
AB-113	769.23	0.0755	0.9586	74.06	1.69	0.9730

Table 5
Kinetics parameters for adsorption of acid dyes on SBA-3/PEHA.

Dye	Pseudo-first kinetic			Pseudo-second-order kinetic		
	q_e (mg/g)	K_1 (L min^{-1})	R^2	q_e (mg/g)	K_2 (g/mg min)	R^2
AG-28	95.43	0.0367	0.9789	285.71	1	0.9907
AY-127	329.21	0.0757	0.9989	476.19	4.9	0.9998
AR-114	216.30	0.0877	0.9992	454.54	7.4	0.9998
A0-67	104.93	0.0557	0.9900	434.78	1.05	0.9998
AB-113	181.27	0.0630	0.9763	500	2.5	0.9882

Where q_e and q_t are the adsorption capacities at equilibrium and at time t, respectively (mg g^{-1}); k_1 is the rate constant of pseudo-first order adsorption (L min^{-1}).

The pseudo-second-order equation of McKay can be represented in the following form [51]:

$$\frac{t}{q_t} = \frac{1}{K_2 q_e^2} + \left(\frac{1}{q_e}\right)t \quad (6)$$

Where the pseudo-second-order constants k_2 (g (mg min)$^{-1}$), and the equilibrium adsorption capacity q_e can be determined experimentally from the slope and intercept of the plot t/q_t versus t. From Table 5, it is clear that the pseudo-second-order kinetic model gave a better correlation for the adsorption of acid dyes on SBA-3/PEHA compared to the pseudo-first-order model. These results suggest that the rate-limiting step may be chemisorption and that the rate equation follows second-order kinetics.

4. Conclusions

The adsorption of acid dyes by SBA-3 ordered mesoporous silica, ethylenediamine functionalized SBA-3 (SBA-3/EDA), aminopropyl functionalized SBA-3 (SBA-3/APTES) and pentaethylene hexamine functionalized SBA-3 (SBA-3/PEHA) materials was studied in the present work. The textural properties and structural order of the synthesized materials were studied by FT-IR, XRD and nitrogen adsorption–desorption analysis. The characteristic results indicated that the functionalization was successfully done and the pore structure of SBA-3 was almost kept unaltered. The obtained results showed that the adsorption capacity of the adsorbents varied in the order SBA-3/PEHA > SBA-3/APTES > SBA-3/EDA > SBA-3. The adsorption capacity of acid dyes by mesoporous silica was enhanced through functionalization with amine groups. SBA-3/PEHA has been demonstrated to be highly effective for the removal of the acid dyes with an adsorption equilibrium time of less than 60 min. The higher adsorption capacity of SBA-3/PEHA may be explained due to the fact that it proceeds via electrostatic interaction and hydrogen bond formation between the surface of the adsorbent and acid dyes. The solution pH played a significant role in influencing the capacity of an adsorbent towards acid dyes molecules. A decrease in the pH of solutions led to a significant increase in the adsorption capacity of SBA-3/PEHA. Higher adsorption capacity is obtained at 20 °C and it decreases with increase in temperature. It is observed that Freundlich isotherm is found to be more suitable and appropriate model to explain the adsorption isotherm of acid dyes on SBA-3/PEHA. The pseudo-first order and pseudo-second-order kinetic models were used to analyze the data obtained for acid dyes adsorption onto the SBA-3/PEHA. The results exhibited that the pseudo-second-order equation provided the better correlation for the adsorption data.

Acknowledgement

The authors are thankful to Research Council of Iran University of Science and Technology (Tehran) for financial support to this study.

References

[1] Chen S, Zhang J, Zhang C, Yue Q, Li Y, Li C. Desalination 2010;252:149.
[2] Pugazhenthiran N, Ramkumar S, Kumar PS, Anandan S. Microporous Mesoporous Mater 2010;131:170.
[3] Crini G. Bioresour Technol 2006;97:1061.
[4] Wang Z, Xiang B, Cheng R, Li Y. J Hazard Mater 2010;183:224.
[5] Lee J-W, Choi S-P, Thiruvenkatachari R, Shim W-G, Moon H. Dyes Pigm 2006; 69:196.
[6] Oei BC, Ibrahim S, Wang S, Ang HM. Bioresour Technol 2009;100:4292.
[7] Jalil AA, Triwahyono S, Adama SH, Rahima ND, Aziz MAA, Hairomc NHH, et al. J Hazard Mater 2010;181:755.
[8] Cheung WH, Szeto YS, McKay G. Bioresour Technol 2009;100:1143.
[9] Malik PK, Saha SK. Sep Purif Technol 2003;31:241.
[10] Koch M, Yediler A, Lienert D, Insel G, Kettrup A. Chemosphere 2002;46:109.
[11] Panswed J, Wongchaisuwan S. Water Sci Technol 1986;18:139.
[12] Ciardelli G, Corsi L, Marucci M. Resour Conserv Recycl 2000;31:189.
[13] Wu FC, Tseng RL. J Hazard Mater 2008;152:1256.
[14] Thinakaran N, Baskaralingam P, Pulikesi M, Panneerselvam P, Sivanesan S. J Hazard Mater 2008;151:316.
[15] Wang S, Zhu ZH. J Hazard Mater 2006;136:946.
[16] Anbia M, Lashkari M. Chem Eng J 2009;150:555.
[17] Anbia M, Mohammadi N, Mohammadi K. J Hazard Mater 2010;176:965.
[18] Anbia M, Ghaffari A. Appl Surf Sci 2009;255:9487.
[19] Anbia M, Mohammadi N. Desalination 2009;249:150.
[20] Anbia M, Mohammadi K. Asian J Chem 2009;21:3347.
[21] Anbia M, Mohammadi K. Chin J Chem 2008;26:2051.
[22] Anbia M, Moradi SE. Chem Eng J 2009;148:452.
[23] Anbia M, Moradi SE. Appl Surf Sci 2009;255:5041.
[24] Anbia M, Khosravi F. Radiat Eff Defects Solids 2009;164:541.
[25] Anbia M, Rofouei MK, Husain SW. Asian J Chem 2007;19:3862.
[26] Anbia M, Harriri SA, Ashrafizadeh SN. Appl Surf Sci 2010;256:3228.
[27] Anbia M, Hariri SA. Desalination 2010;26:61.
[28] Qin Q, Ma J, Liu K. J Hazard Mater 2009;162:133.
[29] Asouhidou DD, Triantafyllidis KS, Lazaridis NK, Matis KA. Colloids Surf A 2009; 346:83.
[30] Posada JA, Cardona CA, Giraldo O. Mater Chem Phys 2010;121:215.
[31] Kresge CT, Leonowicz ME, Roth WJ, Vartuli JC, Beck JS. Nature 1992;359: 710.
[32] Mattigod S, Feng X, Fryxell GE, Liu J, Gong M. Sep Sci Technol 1999;34:2329.
[33] Zhao DY, Huo QS, Feng JL, Chmelka BF, Stucky GD. J Am Chem Soc 1998;120: 6024.
[34] Firouzi A, Kumar D, Bull LM, Besier T, Sieger P, Huo Q, et al. Science 1995;267: 1138.
[35] Huo QS, Margolese DI, Ciesla U, Feng PY, Gier TE, Sieger P, et al. Nature 1994; 368:317.
[36] Che S, Garcia-Bennett AE, Yokoi T, Sakamoto K, Kunieda H, Terasaki O, et al. Nat Mater 2003;2:801.
[37] Zhao D, Feng J, Huo Q, Melosh N, Fredrckson G, Chmelka B, et al. Science 1998; 279:548.
[38] Chen F, Xu X-J, Shen S, Kawi S, Hidajat K. Microporous Mesoporous Mater 2004;75:231.
[39] Albouy PA, Ayral A. Chem Mater 2002;14:3391.
[40] Lee JS, Joo SH, Ryoo R. J Am Chem Soc 2002;124:1156.
[41] Feng X, Fryxell GE, Wang LO, Kim AY, Liu J, Kemner KM. Science 1997;276: 923.
[42] Lim MH, Stein A. Chem Mater 1999;11:3285.
[43] Huo Q, Margolese D, Stucky GD. Chem Mater 1996;8:1147.
[44] Nowinska K, Formaniak R, Kaleta W, Waclaw A. Appl Catal A 2003;256:115.
[45] Goltner CG, Smarsly B, Berton B, Antonietti M. Chem Mater 2001;13:1617.
[46] Yakup Arıca M, Bayramoglu G. J Hazard Mater 2007;149:499.
[47] Langmuir I. J Am Chem Soc 1918;40:136.
[48] Freundlich HMF. J PhysChem 1906;57:385.
[49] Sharma A, Bhattacharyya KG. Adsorption 2004;10:327.
[50] Ho YS, Ng JCY, McKay G. Sep Purif Methods 2000;29:189.
[51] McKay G, Ho YS. Process Biochem 1999;34:451.